Open Journal of Modern Hydrology, 2022, 12, 32-54
https://www.scirp.org/journal/ojmh
ISSN Online: 2163-0496
ISSN Print: 2163-0461

# Oxbow Lakes as Geological Archives of Historical Changes in Channel Substrate, Swan Creek, Toledo, Ohio (USA)

**Jocelyn L. Hicks, James E. Evans**

Department of Geology, School of Earth, Environment, and Society, Bowling Green State University, Bowling Green, OH, USA
Email: evansje@bgsu.edu

**How to cite this paper:** Hicks, J.L. and Evans, J.E. (2022) Oxbow Lakes as Geological Archives of Historical Changes in Channel Substrate, Swan Creek, Toledo, Ohio (USA). *Open Journal of Modern Hydrology*, **12**, 32-54.
https://doi.org/10.4236/ojmh.2022.122003

**Received:** February 9, 2022
**Accepted:** March 12, 2022
**Published:** March 15, 2022



## Abstract

Efforts to restore urban rivers require an understanding of human-influenced changes in channel substrates. This study uses three naturally-occurring oxbows in a 3.5 km reach of Swan Creek, flowing through the City of Toledo, Ohio (USA) to reconstruct historical changes in channel substrate. Human impacts in the watershed were: 1) land clearance for agriculture (peaking in 1900-1920) and for suburban housing tracts (peaking in 1945-1970), followed by 2) the post-1940 creation of more efficient urban run-off systems from streets, parking lots, housing developments, and shopping centers. Historical aerial photographs and maps from 1935, 1940, 1950, 1963, 1974, and 1994 were georeferenced using ground control points, input to ArcGIS, and have root mean square error (RMSE) ranging from 0.19 - 0.77 m (average RMSE = 0.47 ± 0.20 m) when compared to the 2006 digital ortho quarter-quadrangle (DOQQ) image used as the basis for comparison. Results showed that channel sinuosity continually increased from 1.88 (1935) to 1.99 (2006). Two oxbows probably formed in 1913, and the third formed in 1940. Sediment cores and trenches were used to recognize historical channel substrates. Age control was provided by $^{14}C$ geochronology and labels on food packaging materials found in flood layers. Grain-size analysis of channel substrates shows a historical coarsening-upward trend: the largest clast size interval ($\phi_5$) changes from $+0.78\phi$ in pre-1935 channels, to $-1.15\phi$ in pre-1940 channels, to $-1.69\phi$ in the 2006 channel. These results indicate recent urban runoff created fluvial pavements and increasing channel mobility as the stream removes legacy sediment from intrabasinal sediment storage.

## Keywords

Oxbows, Channel Substrate, Legacy Sediment, Anthropogenic Change, Sediment Budget

# 1. Introduction

## 1.1. Purpose

River channels can shift location through lateral channel migration (erosion at the cutbank and deposition on the point bar), through chute cut-offs (re-occupation of a former chute channel crossing the point bar, followed by abandonment of the previous channel), through neck cut-offs (intersection of meander loops, followed by abandonment of the previous channel) and through avulsion (levee breaching and crevasse splay evolution, followed by abandonment of the previous channel). The last three of these channel migration processes can produce oxbows or abandoned channels (this paper will use the terms synonymously). The properties of such abandoned channels are the focus of this paper.

Each oxbow has a sedimentary infill history which can be observed in a vertical stratigraphic section (such as a sediment core or trench). The lowest portion of abandoned channel fills consists of coarse-grained sediment (gravel, coarse-grained sand, and shell fragments), deposited by bedload transport through the active channel prior to the cut-off event. These former fluvial channel deposits represent the channel substrates that existed at the time of channel cut-off and abandonment. The channel substrates are overlain by finer-grained deposits (fine-grained sand, silt, mud, and peat) deposited after the oxbow has been disconnected from the active channel.

The infill of an abandoned channel varies spatially. Sand accumulates at the junction between the abandoned channel and active channel, effectively plugging the mouth of the abandoned channel [1] [2]. Farther away from this junction, the abandoned channel evolves through an initial lacustrine phase (oxbow lake) that is gradually infilled by lacustrine gyttjas interbedded with episodically deposited, flood-generated, suspension-load sediments [3] [4]. Over time, the interbedded flood deposits become less frequent and represent only the higher magnitude flooding events, because the abandoned channel becomes more spatially disconnected from the active channel [5]. Finally, the abandoned channel evolves from an oxbow lake into a riparian wetland, infills with peat, and is capped by organic-rich soils (histosols).

Abandoned channels have long been of interest. Previous workers have discussed how the morphology and infill of abandoned channels in the geologic record allow for the reconstruction of flow parameters about ancient streams [6] [7]. The properties of oxbows in the Murrumbidgee River basin, Australia, have been used to reconstruct historical changes in hydrologic regime [8]. Bed elevations and sediment characteristics from abandoned channels along the Hunter River, Australia, have been used to reconstruct changes in flood history and sediment loads due to human activity and climate change [9]. The contaminant history of the Deûle River, France, has been reconstructed from oxbow lake sediment cores [10]. The evolution of oxbows along the Ain River, France, particularly their silting-up history, has been used to evaluate the longevity of riparian wetlands [11]. Previous studies calculated historical sediment accumulation rates from oxbow sediment cores in Mississippi, and matched those to changes in agricultural land-use practices [12]. Detailed analysis of sediment cores from abandoned channels of the Sandusky River, Ohio, in a rural agricultural setting, has shown how changes in specific agricultural crop types and agricultural best management practices (BMPs) affected historical sediment loads [13]. The effects of dam construction and hydraulic engineering on the Ottawa River, Ohio, have been determined by studying changes in channel substrates in an abandoned channel [14].

This study evaluates the impact of human land-use modification (land clearance and urbanization) on river channel substrate in an urban area, using abandoned channel deposits as a geological archive. The study first evaluates changes in river morphology, using historical aerial imagery and maps from 1935-2006 to reconstruct the history of naturally occurring cut-offs on Swan Creek (northwest Ohio, USA). The history of these oxbows is then related to land-use change in the watershed. Finally, the sediment properties of these oxbows are evaluated to determine changes in channel substrates, which are also linked to land-use change. Oxbow lake sediments represent an archive for reconstructing historical changes in urban rivers, and provide key data for urban river restoration.

## 1.2. Background

### 1.2.1. Study Area

Swan Creek is a river in northwest Ohio, which flows through the southern part of the Toledo metropolitan area (**Figure 1(A)**). This river is a tributary for the Maumee River, which flows into Lake Erie, one of the Laurentian Great Lakes of North America. The study area was selected from a natural area preserve, called Swan Creek Metro Park, because of minimal land-use modification allowing for recognition of older fluvial geomorphic features. Three oxbow lakes were identified within the study area (**Figure 1(B)**).

The study area contains three fluvial terraces and a relatively small modern floodplain. The two upper terraces (T1 and T2) formed during deglaciation phases of a series of glacial lakes that preceded modern Lake Erie [15]. The lowest terrace (T3) is only slightly elevated above the modern floodplain, and studies on similar features near the study area have shown T3 to be an anthropogenic terrace consisting of legacy sediment that formed due to excess sediment supply linked to land clearance in the region between about 1850-1970 [14] [16].

The upper T1 terrace extends over a large upland area, and was converted from forest to agriculture during the late-1800s. Within the study area itself, the T1 terrace area was once part of a state-run dairy farm and maintained as pasture [17]. During about 1945-1970, agricultural land throughout the region was converted to housing developments, in accord with the suburbanization of most American cities at this time (**Figure 2**). With surrounding land conversion to urbanization, the dairy farm was closed, the land designated as a park owned by Lucas County, to serve the residents of the City of Toledo, and efforts made to reforest much of the park. In addition, urban drainage systems were installed post-1940 to handle run-off.

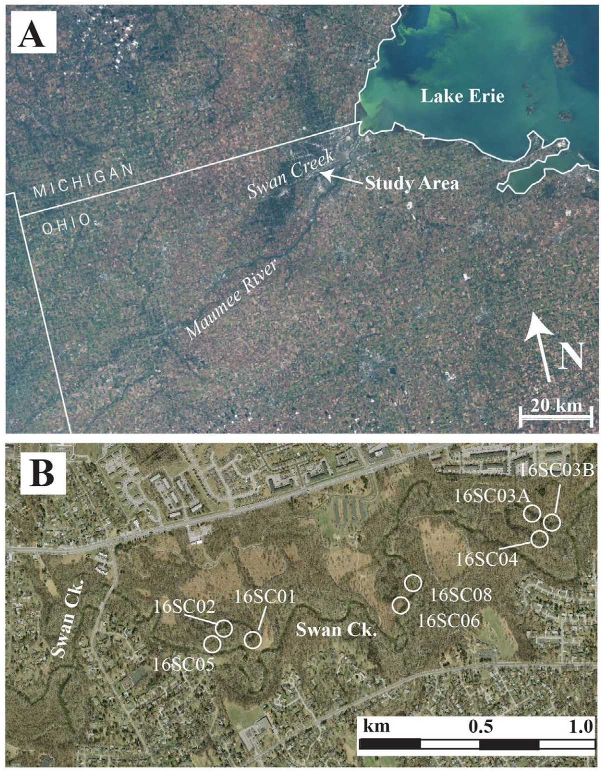


**Figure 1.** (A) Location map showing northwest Ohio, Lake Erie, the Maumee River, and the study area on Swan Creek. (B) Aerial image from 2006 showing the location of the three oxbows and the locations of trenches and sediment cores used in this project.

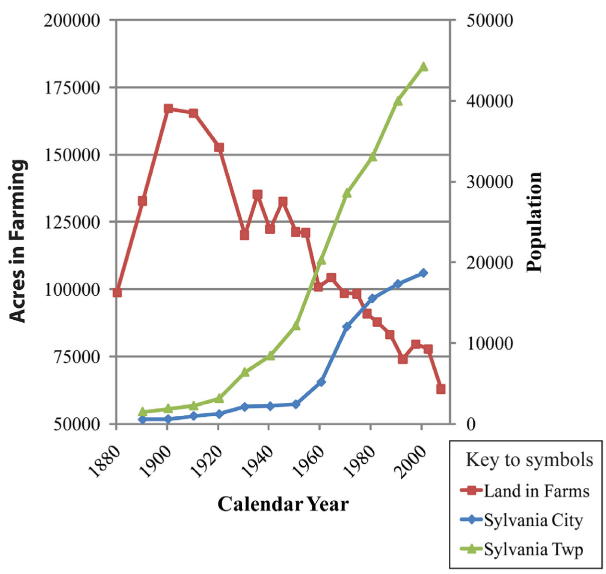


**Figure 2.** Graph showing calendar year (X-axis) versus historical trends in land area used for farming (Y-axis left) and human population (Y-axis right) in the vicinity of the drainage basin.

#### 1.2.2. Ecology and Land-Use

Prior to the arrival of European settlers in the 1800s, this region was part of the Great Black Swamp, an extensive wetland area which was a mosaic of ash-swamp elm wetland forest, wetlands, wet prairie, and oak savanna forest [18] [19] [20]. The region has some of the last portions of the State of Ohio to be deforested for agriculture because it required the development of steam-powered ditching equipment, use of tile drains, and a legal framework for the priority of drainage ditches across private land [21] [22]. Reduction of the original swamp forest was accomplished in a relatively narrow time window (1880s-1890s), facilitated by the introduction of railroads and roads through the swamp [23]. Currently, the study area is mostly covered by second-growth forest less than about 100 years old.

#### 1.2.3. Hydrology

Swan Creek is a tributary of the Maumee River, and joins the Maumee River 9.5 km downstream of the study area. Upstream of its terminus, Swan Creek flows semi-parallel to the Maumee River, and the two have almost identical slopes (3.4 m/km for Swan Creek versus 3.2 m/km for the Maumee River). Swan Creek does not have a permanent United States Geological Survey (USGS) stream gaging station, but there was a temporary gaging station near the study area which operated between 2015-2017 (USGS gage station #04193999). In contrast, on the Maumee River at Waterville (14 km distant) is a permanent USGS gage station (#04193500) with a continuous record from 1898-2022.

In order to create an artificial hydrograph record for the study area on Swan Creek, we compared the 2015-2017 stream flow data from the two USGS gage stations (**Figure 3**). It can be shown that the minimum and maximum flow peaks for Swan Creek and the Maumee River have been contemporaneous. This permitted constructing a proxy hydrologic record for Swan Creek [24]. From this proxy record, it can be shown that the twenty largest flow events of record between 1898-2006 (in order of magnitude) occurred during: 1913, 1982, 1985, 2005, 1950, 1978, 1991, 1981, 1959, 1966, 1943, 1999, 1930, 1974, 1944, 1969, 1993, 1976, 1994, 1997, and 1940. Most major floods occur in the spring (January to March) due to snow melt or rain on impermeable surfaces such as ice. There is a historical trend toward more frequent major floods. For the 123-year record over the interval 1898-2022, 23 of the largest 35 flood events have occurred since 1970.

## 2. Methods

### 2.1. Field Methods

This study used a combination of trenches, push cores, and vibracores to evaluate the sedimentology and stratigraphy of abandoned channels in the study area. Six trenches were dug using shovels and pickaxes. The surface of the exposure was cleaned, photographed, described, and sampled for textural analysis. The exposed stratigraphy in each trench was extended using push cores (4.5 cm

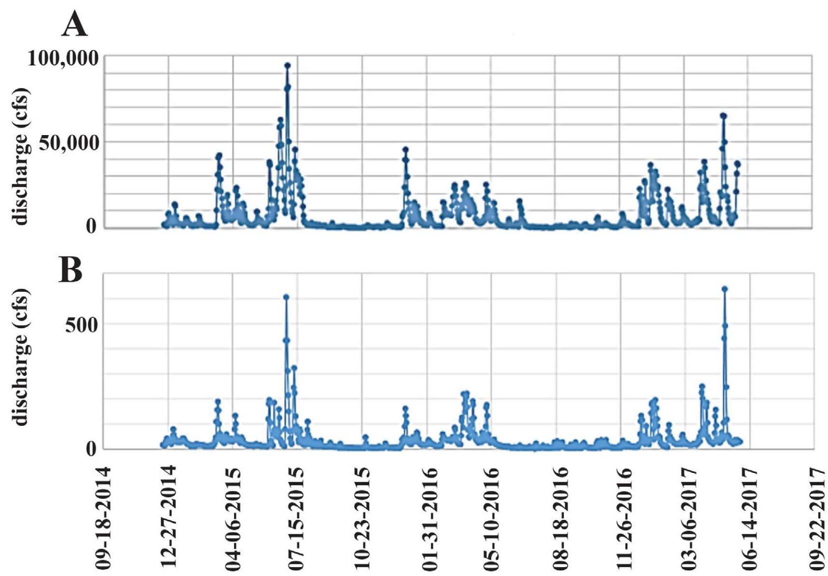


**Figure 3.** Comparison of gage station data, showing (A) a portion of the 1898-2022 record from the USGS gaging station on the Maumee River at Waterville (#04193500) and (B) the 2015-2017 record from the temporary USGS gaging station on Swan Creek. The 2015-2017 similarity in flow records from these two gage stations, located 14 km apart, allowed for the creation of a synthetic hydrograph record for the study area.

diameter Lexan core tubes) at the base of the trench. When trenches exposed wood debris or bivalve shells at depth, samples were collected for $^{14}C$ geochronology. In addition, trenches exposed anthropogenic artifacts (food packaging materials) deposited in certain layers. These were collected to determine if any of this material had geochronology value. In addition to trenches, vibracores (7.5 cm diameter aluminum core tubes) were collected at several locations within historical oxbows. Finally, modern channel cross sections were sampled to collect bedload sediment comprising the existing channel substrate [24].

## 2.2. Laboratory Methods

In the laboratory, sediment cores were split in half lengthwise, one section archived and the other section used as the working half for subsequent analysis. The working half of the core was cleaned, photographed, and described. Sediment color was identified using the Munsell color chart [25]. Sand and gravel layers in the working half of each core were sampled for grain size analysis.

Samples for grain size were washed in distilled water, dried in a drying oven at 90˚C, and gently agitated to mechanically separate any clumped grains. Samples were then sieved through a nest of sieves on a shaking platform, weighed to determine mass, and the data plotted on histograms and cumulative frequency plots. Calculated grainsize statistics included the mode, median, mean, standard deviation and skewness of each sample [26].

Three samples were evaluated using $^{14}C$ geochronology [27]. A freshwater mollusk shell and a separate piece of wood were recovered from the same stratigraphic layer in trench 16SC5. A piece of wood was also recovered from trench 16SC8. All three were evaluated by the Direct AMS Laboratory (Seattle, Washington). The ages were converted to calendar year before present (cal. yr B.P.) using radiocarbon calibration program Calib revision 7.1.® [28], with the $\delta^{13}C$ corrections Marine$^{13}$ used for the shell sample and INTCAL$^{13}$ used for the wood samples [29]. This program produces a probability distribution, and from this a mean and standard deviation ($1\sigma$) are herein reported. Detailed explanations are given elsewhere [24].

### 2.3. Image Analysis

This study used historical aerial imagery provided by the United State Geologic Survey (USGS), Ohio Geographically Referenced Information Program (OGRIP), and the City of Toledo (**Table 1**). Historical aerial images were available from 1940, 1950, 1963, 1974, and 2006. The 2006 digital ortho quarter quadrangle (DOQQ) image was used as a base map in this study because it was previously georectified. In order to compare images from different time periods, the historical aerial photographs were digitized and imported into ArcGIS® version 10.3 [30]. The four older images were georeferenced by first identifying ground control points (GCPs) such as road intersections, buildings, and railroad crossings. The GCPs from these historical aerial photographs were then matched to corresponding GCPs in the 2006 DOQQ using the georeferencing tool in ArcGIS, following the stepwise method [31]. The root mean square errors (RMSE) are shown in **Table 1**. Details of the methodology are provided elsewhere [24]. In addition to historical aerial photographs, the 1935 and 1994 USGS topographic maps were evaluated using the identical technique.

**Table 1.** Aerial photograph data base.

| Date Acquired | Source | Image Format | Designation | RMS Error (m) |
|---|---|---|---|---|
| 5-23-1940 | City of Toledo | Black-and-White | BVG-1-23 | 0.27 |
| 5-23-1940 | City of Toledo | Black-and-White | BVG-1-26 | 0.38 |
| 8-24-1950 | City of Toledo | Black-and-White | BVG-2G-151 | 0.78 |
| 8-24-1950 | City of Toledo | Black-and-White | BVG-2G-153 | 0.70 |
| 5-2-1963 | City of Toledo | Black-and-White | BVG-2DD-237 | 0.43 |
| 5-2-1963 | City of Toledo | Black-and-White | BVG-2DD-239 | 0.52 |
| 4-28-1974 | City of Toledo | Black-and-White | 9-12 | 0.50 |
| 4-28-1974 | City of Toledo | Black-and-White | 10-10 | 0.20 |
| 2-3-2006 | OGRIP | DOQQ | | Base Image |

**Explanation:** Multiple images are listed for 1940, 1950, 1963, and 1974 because the study area overlapped two frames. The City of Toledo, Ohio, is a metropolitan governmental unit. It probably obtained the 1940, 1950, and 1963 images from the USDA-NRCS (U.S. Department of Agriculture, Natural Resources Conservation Service). OGRIP is the Ohio Geographically Referenced Information Program (State of Ohio). DOQQ is a Digital Ortho Quarter Quadrangle images rectified to an existing statewide 2.5 foot DEM.

There were two problems in using the above methods to identify historical channel positions. First, tree canopy cover blocked the position of the channel banks on portions of certain images. The extent of this tree canopy interference depended on the season of year that the original aerial imagery was collected. This problem was mitigated by comparing the blocked areas on any particular image to the corresponding locations on older and more recent images, which for many cases confirmed that there was no change in river channel position at this location [31]. The second problem is that the oldest available aerial imagery only dated to 1940. In order to extend the historical record, the 1935 USGS topographic map was also digitized and georeferenced. This topographic map showed the geographic position of the river, but because it probably involved field estimates of river channel width, the resulting GIS shapefile for the 1935 channel appears much wider than is probably realistic, which may introduce error into the 1935 channel reconstruction.

A digital elevation model (DEM) of the study area was constructed in an effort to identify subtle topographic features, such as additional abandoned channels. The DEM construction method is explained in more detail elsewhere [24]. The Jenks classification was used to identify the natural breaks in the dataset by grouping similar values in a manner that maximizes the difference between the breaks [32]. The analysis correctly identified the locations of the three terraces and the three oxbows evaluated in this study, but the method apparently did not have sufficient resolution to identify additional meander scars or oxbows, so it will not be discussed further.

## 3. Results

### 3.1. Historical Channel Positions

The georeferenced channel positions for 1935, 1940, 1950, 1963, 1974 and 2006 are shown as maps in **Figure 4**. The three abandoned channels are shown in colors (red, green, and blue). The 1935 channel map differs from the others in two regards: 1) because it was based on a topographic map, the channel GIS shapefiles show channel width that is unrealistically wide, and 2) the most recent oxbow lake is not shown in the image because it was part of the 1935 channel. The 1940 channel map shows that a cut-off and channel abandonment event occurred between 1935-1940. The subsequent imagery shows lateral channel migration, but no additional cut-offs between 1940-1994. The 2006 image shows the initial stages of a chute cut-off that was in progress, but this channel cut-off and abandonment has still not occurred by 2022. The modern channel is incised, and lateral channel migration occurs primarily due to channel bank slump failures. The in-progress chute cut-off appears related to the flow diversion effect of an upstream log jam, and resulting bank failure.

The process of overlying historical aerial photographs can be used to compare and measure differences between the channel morphologies at different times. In order to determine this, the center of each bend was identified. Sinuosity was

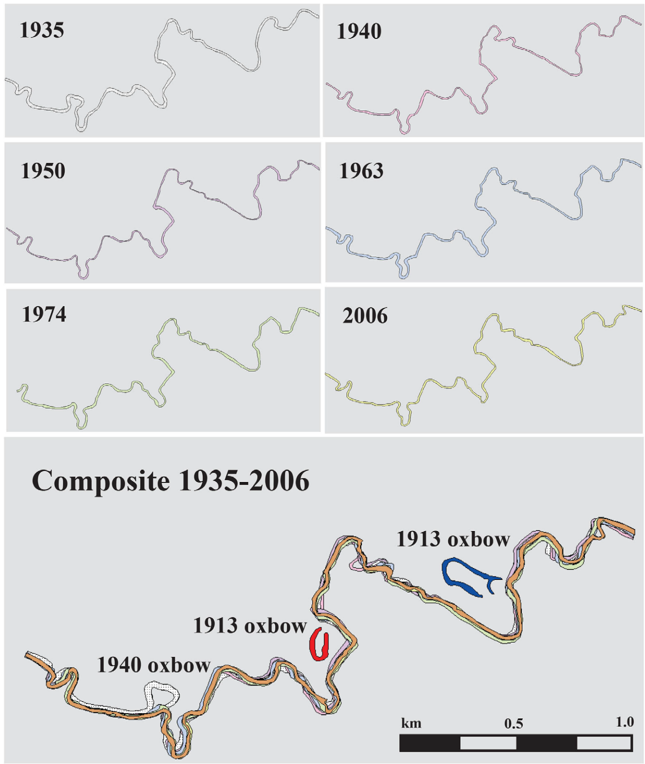


**Figure 4.** Georeferenced channel positions for 1935, 1940, 1950, 1963, 1974, and 2006. The composite for 1935-2006 overlays all of the historical aerial images. See text for details.

calculated as the ratio between channel thalweg distance and direct path distance between adjacent meander bends. The results (**Table 2**) show that channel sinuosity has continually increased from 1.88 in 1935, to 1.99 in 2017.

## 3.2. Facies Analysis

Evaluation of trenches and cores led to recognition of twelve (12) different lithofacies (**Table 3**). Each lithofacies represents a unique combination of composition, texture, and sedimentary structures, and are interpreted to represent specific depositional processes. Lithofacies can be grouped into lithofacies associations using the following criteria: 1) lithofacies that form a fining-upward succession, 2) lithofacies that form a coarsening-upward succession, 3) lithofacies that alternate repetitively, and/or 4) lithofacies that are separated from others by an erosional surface. This study found four lithofacies associations (**Table 4**), which represent sub-environments in an overall fluvial depositional environment.

### 3.2.1. FA1: Fluvial Channel-Fill Facies Association

Fluvial channel-fill deposits are recognized from a basal erosional surface, the presence of massive, fine-grained gravels or pebbly sands composed of pebbles, granules, and shell fragments (lithofacies Gm), overlain by massive sand (lithofacies Sm) and/or laminated sand (lithofacies Sl), and capped by massive silts (lithofacies SSm) or massive muds (lithofacies Mm). The basal erosional surface is interpreted as the base of the fluvial channel. The overlying sands and gravels are interpreted as bedload deposits transported through that fluvial channel. Those sands and gravels would have represented the substrate of the active fluvial channel. Shell fragments are pieces of freshwater bivalves from species still present in the active channel. As observed in the modern channel, the bedload deposits most likely were originally found in fluvial bedforms such as rippled sand sheets, sand dunes, and sandy gravel bars. Presumably, the massive sand deposits (lithofacies Sm) initially had sedimentary structures such as ripple lamination and cross bedding, but such sedimentary structures were indistinct in our trenches and cores. The sand and gravel deposits forming the basal channel substrates ranged from 15 - 50 cm thick.

**Table 2.** Historical changes in sinuosity through study reach.

| Data Year | Thalweg Length (m) | Direct Path Length (m) | Sinuosity |
|---|---|---|---|
| 1935 | 1534.695 | 815.776 | 1.881 |
| 1940 | 1590.541 | 819.744 | 1.940 |
| 1950 | 1596.664 | 816.769 | 1.955 |
| 1963 | 1608.414 | 821.649 | 1.958 |
| 1974 | 1612.301 | 821.917 | 1.962 |
| 2006 | 1632.204 | 822.179 | 1.985 |

**Explanation:** Sinuosity is the ratio of thalweg path length to direct (down valley) path length.

**Table 3.** Lithofacies descriptions.

| Code | Lithology | Textures | Sedimentary Structures | Interpretation |
|---|---|---|---|---|
| Gm | Gravel | Pebbles, shells | Massive | Channel base (substrate) |
| Sl | Sand | Fine-grained | Planar laminated | Channel-fill (bar top) |
| Sm | Sand | Fine-grained | Massive | Channel-fill (dunes?) |
| Smf | Sand | Very fine-grained | Massive with mud lenses | Proximal overbank |
| Smo | Sand | Very fine-grained | Massive with wood debris | Proximal overbank |
| SSm | Silt | Coarse-grained | Massive | Distal overbank |
| SSmr | Silt | Coarse-grained | Massive, rooted (soil) | Distal overbank (soil) |
| Ml | Mud | Silt and clay | Laminated | Oxbow lake flood layer |
| Mm | Mud | Silt and clay | Massive | Oxbow lake infill |
| Mmo | Mud | Silt, clay, organics | Massive | Lacustrine gyttja |
| Mmr | Mud | Silt and clay | Massive, rooted (soil) | Distal overbank (soil) |
| O | Peat | Fibrous peat | Massive | Wetland histosol (soil) |

**Explanation:** Lithofacies Sm (massive, fine-grained sand) may have originally had cross-bedding or other sedimentary structures, but these are indistinct in trenches and cores.

Table 4. Lithofacies associations.

| Name | Lithofacies | Thickness | Organization | Interpretation |
|---|---|---|---|---|
| FA1 | Gm, Sm, Sl, SSm, Mm | Up to 2.5 m | Lenticular, Ribbon | Modern or abandoned lenticular channel overlying erosional scour surface |
| FA2 | Mmo, Ml, SSm, Mm | 0.5 to 1.2 m | Lenticular, Ribbon | Abandoned channel, lacustrine phase with frequent interbedded flood deposits |
| FA3 | O, SSm, Mm | Up to 0.5 m | Lenticular, Ribbon | Abandoned channel, wetland phase (peat), with rare interbedded flood deposits |
| FA4 | Smf, Smo, SSm, SSr, Mm, Mmr | 0.3 to 1.3 m | Wedge, Sheet | Overbank deposits, thinning away from channel, soils |

**Explanation:** For lithofacies codes, see Table 3. Organization refers to cross-sectional view and map view.

Each channel-fill succession may be truncated or overlain by another channel-fill sequence, or else overlain by fine-grained deposits from the lacustrine facies association, wetlands facies association, or overbank facies association (each discussed below). The succession from channel-fill facies association to lacustrine facies association to wetland facies association is interpreted as a channel abandonment succession representing the infill history of an oxbow lake. Complete channel abandoned successions average 2.0 to 2.5 m in thickness, which can be directly compared to the modern channel nearby, and which approximates bankfull channel depth in the active channel.

#### 3.2.2. FA2: Lacustrine Facies Association

Thick deposits of massive organic-rich muds or gyttjas (lithofacies Mmo) are interpreted as oxbow lake deposits. The gyttjas can contain terrestrial gastropod shells and wood fragments. Typically, these were interbedded with thin layers or laminae of massive silt (lithofacies SSm), laminated silty-clay (lithofacies Ml) or massive silty-clay (lithofacies Mm). These silt-rich layers or laminae, within the oxbow lake succession, are interpreted as flood deposits that sourced from the suspension load of the active channel. Overall, the lacustrine facies succession varies from 0.5 - 1.2 m thick.

The lacustrine facies association directly overlies the fluvial channel-fill facies association described above. The contact is abrupt and non-erosional. There is typically a notable color change from gray sands and gravels to dark brown gyttjas corresponding to the contact. The top of the lacustrine succession gradually transitions either into peats (wetlands facies association) or laminated silts and clays (overbank facies association). In many cases, the upper parts of the lacustrine succession consist of silts and muds that are disturbed by plant roots (lithofacies SSmr and Mmr).

#### 3.2.3. FA3: Wetlands Facies Association

A wetland sequence can be recognized by the presence of fibric peat deposits (lithofacies O) up to 0.5 m thick. Accumulations of peat represent both the accumulations of organics (influx and decay of terrestrial organic matter) but also the geographical exclusion of mineral sediment, such as suspension load sediments from the active channel. The most effective peat-forming environments escape clastic sediment contamination by upwards growth above flood stage (domed peats) or because of a barrier blocking flood waters from reaching the site of peat accumulation [33]. In this case neither mechanism applies, and these peats incorporate clastic materials and are interbedded with clastic flood deposits (lithofacies SSm, Mm, and/or Ml).

#### 3.2.4. FA4: Overbank Facies Association

These deposits consist of massive very fine-grained sands with mud lenses (lithofacies Smf), massive sands with wood debris (lithofacies Smo), massive silts (lithofacies SSm), and massive muds (lithofacies Mm). In the modern floodplain, these deposits form a sheet-like deposit with variable thickness, wedging out laterally away from the active channel. Many of the deposits are rooted, and incorporated into soils (lithofacies SSmr and Mmr). These overbank deposits range from 0.3 to 1.3 m thick, and can overlie any of the previous lithofacies associations previously described.

### 3.3. Stratigraphy and Geochronology

The alluvial stratigraphy of the study area, as shown in cores and trenches, varied spatially. Overall, the infill of abandoned channels reliably consisted of a scoured surface, representing the base of the former channel, overlain by pebbly sands or gravels (FA1) representing the formerly active channel bedload component, overlain by some combination of oxbow lake sediments (FA2), riparian wetland sediments (FA3), and/or overbank flood deposits (FA4), and capped with modern soils. The thickness of the abandoned channel infill was 2.0 to 2.5 m, which is equivalent to bankfull depth of the nearby active channel.

An example of an abandoned channel infill succession is shown in **Figure 5**. This image shows the trench near the pre-1940 oxbow (16SC5). In addition to an image of the 200-cm deep trench (**Figure 5(A)**), there is an image of the 41-cm pushcore taken from the bottom of the trench (**Figure 5(B)**) and the composite 241-cm stratigraphic section (**Figure 5(C)**).

The composite section begins with the upper portion of a channel succession (≥4 cm lithofacies Gm and 8 cm lithofacies Sl) overlain by 23 cm of overbank deposits (lithofacies Ml and Mm). The abandoned channel that is the focus for this study starts at the top of the push core (6 cm lithofacies Gm) which overlaps with the base of the trench (56 cm lithofacies Gm). The channel cutoff occurred at the gray to brown color transition (arrow) immediately above the 40-cm long shovel. Overlying the abandoned channel succession is an oxbow lake succession 65-cm thick, consisting of lithofacies Smo, Mmo and Ml, with interbedded silty flood layers (lithofacies SSm). The top of the trench is a tan-colored, overbank succession 85-cm thick, consisting of lithofacies Smf, SSm, and Mm, with a modern soil (lithofacies SSmr and Mmr) at the top. The wetland succession (peats) is missing at this location, possibly due to proximity to the active channel.

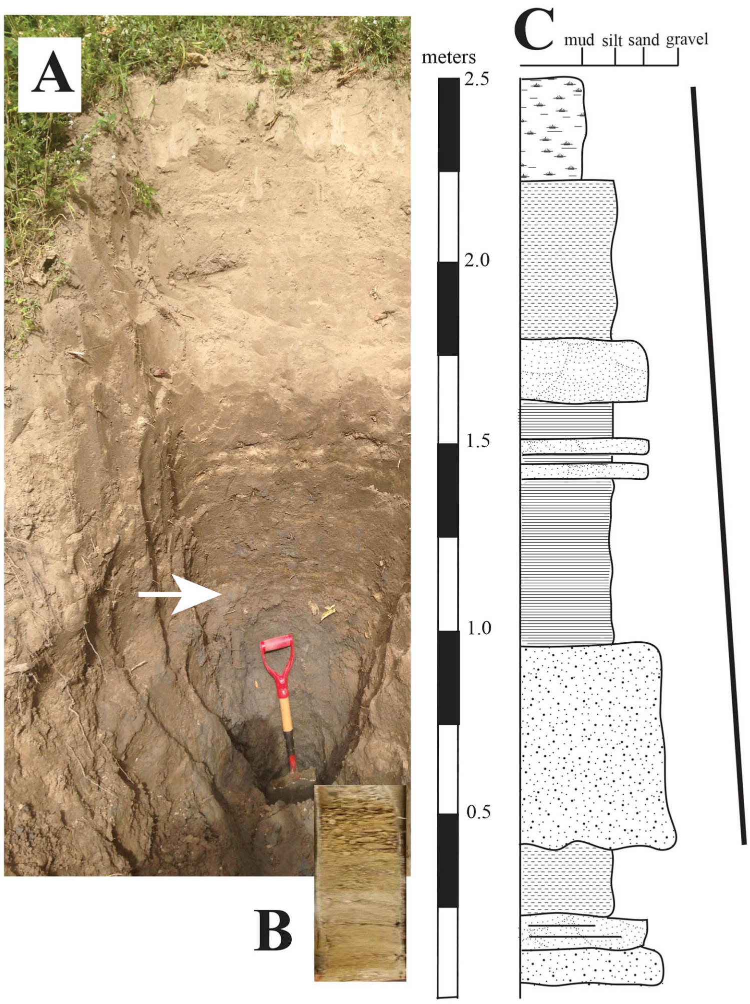


Figure 5. (A) Trench through the 1940 abandoned channel, showing fluvial channel-fill sands and gravels, overlain by oxbow lake deposits, and overbank deposits. (B) Push core taken at the base of the trench. (C) Composite stratigraphic section at this site.

Wood debris found at the base of the oxbow lake succession (circled) has a calibrated $^{14}C$ age of 94 ± 22 cal. yr B.P. or calendar year 1922. This is a maximum depositional age, because it is likely the tree would have died, fallen to a position on the floodplain or stream channel, and remained at some other location(s) prior to being transported to the final depositional location. Because the historical aerial photography shows that this cut-off occurred between 1935 (last imagery showing the location as part of the active channel) and 1940 (earliest imagery showing the cut-off), it can be inferred that the age of the deposit lagged the age of the wood debris by 13 - 18 years.

At other locations, $^{14}C$ geochronology was less useful because of the great age of the material, implying fluvial reworking and remobilization of wood or shell debris. There was greater success with establishing the ages of anthropogenic materials, particularly food packaging materials. For example, one flood layer contained a "MacDonald's BBQ sauce" container top piece with a copyright of 1986. In another case, a flood layer contained a candy wrapper from "Sour War

Heads," and the packaging design and trademark logo constrain this item to 1993-2004. A flood layer contained the lid to a "Pringles' potato chip" container, which was first commercially introduced in 1975. Finally, the design of a "Wendy's crackers" wrapper is constrained to 1983-2013. Establishing the ages of these food wrapping materials required working with each respective company through their historical records departments [24]. It appears humanity is producing numerous useful stratigraphic markers in the geologic record.

### 3.4. Textural Analysis of Modern and Abandoned Channels

Grain size analysis and statistics for the substrates of abandoned channels and the modern channel are presented in **Table 5**. The data are split into three groups: 1) samples from abandoned channels that pre-date the oldest available historical imagery of 1935, 2) samples from the abandoned channel formed by a cut-off that occurred between 1935 imagery and 1940 imagery, and 3) samples from the modern channel. All of the samples share the following characteristics: poorly sorted (standard deviation between $1\phi$ and $2\phi$) and nearly symmetrical skewness (skewness between +0.10 and −0.10).

Otherwise, the most significant observation is that channel substrates become coarser grained over time. For example, the mean and standard deviation changes from $2.83 \pm 1.23\phi$ prior to 1935, to $2.09 \pm 1.76\phi$ between 1935-1940, to $1.11 \pm 1.69\phi$ in the modern channel. The most significant concern is the maximum grain size, because this determines the hydrologic and ecological characteristics of the channel substrate. In this study, we use the 5$^{th}$ percentile ($\phi_5$) of the grain size distribution in phi units as a surrogate for the maximum grain size (note: depending on how cumulative frequency diagrams are plotted, some researchers would call the maximum grainsize $\phi_{95}$ instead of $\phi_5$, but this is conceptually identical). In this study, $\phi_5$ changed from $+0.78\phi$ in pre-1935 channels, to $-1.15\phi$ in pre-1940 channels, to $-1.69\phi$ in the 2006 channel. This represents a transition from coarse-grained sand to granule-pebble grain size, and indicates channel substrate armoring, or the development of fluvial pavements.

## 4. Discussion

### 4.1. Identifying Abandoned Channels in Core and Trenches

Abandoned channels are recognized by the contrast between: 1) gravels and coarse-grained sands, representing the substrate of the active channel, overlain by 2) massive or ripple laminated fine-grained sands, representing levee and proximal channel deposits, overlain by 3) relatively thick deposits of silt and clay, representing overbank or vertical accretion deposits [6] [34] [35]. In addition, the fine-grained infill may be subdivided into a lacustrine phase and subsequent wetland phase, as previously discussed [3] [4].

This study identified historical oxbows using aerial imagery and assigned ages for cut-offs based upon proxy flood records. Subsequent trenching and coring confirmed the presence of abandoned channel successions at these sites. Each abandoned channel succession was approximately the identical thickness (2.0 to 2.5 m) as the bankfull channel depth of the modern channel. The base of each abandoned channel was erosional and overlain by sands and gravels, interpreted as the bedload materials of the formerly active channel. The contrast between the former active channel deposits and infill of the abandoned channel was not only textural, but evident in a color shift from gray to dark brown (Figure 5).

**Table 5.** Textural analysis of abandoned and modern channels.

| Sample | $\phi_5$ | $\phi_{16}$ | $\phi_{50}$ | $\phi_{84}$ | $\phi_{95}$ | Median ($\phi$ units) | Mean ($\phi$ units) | SD ($\phi$) | Skew | Interpretation |
|---|---|---|---|---|---|---|---|---|---|---|
| 16SC3 | −0.2 | 0.9 | 2.4 | 4.1 | 5.1 | 2.4 | 2.47 | 1.60 | 0.04 | Pre-1935 channel |
| 16SC4 | 2.1 | 2.6 | 3.3 | 4.2 | 4.5 | 3.3 | 3.37 | 0.76 | 0.06 | Pre-1935 channel |
| 16SC6 | 0.7 | 1.6 | 2.8 | 4.3 | 4.7 | 2.8 | 2.90 | 1.29 | 0.03 | Pre-1935 channel |
| 16SC8 | 0.5 | 1.3 | 2.5 | 3.9 | 4.5 | 3.9 | 2.57 | 1.26 | 0.04 | Pre-1935 channel |
| 16SC1 | −0.9 | 1.5 | 2.7 | 3.8 | 4.7 | 2.7 | 2.67 | 1.43 | −0.16 | Pre-1940 channel |
| 16SC2 | 1.0 | 1.9 | 3.1 | 4.4 | 5.2 | 3.1 | 3.13 | 1.27 | 0.02 | Pre-1940 channel |
| 16SC5c | −4.0 | −2.3 | 0.3 | 2.8 | 4.2 | 0.3 | 0.27 | 2.52 | −0.03 | Pre-1940 channel |
| 16SC5f | −0.7 | 0.5 | 2.3 | 4.1 | 5.3 | 2.3 | 2.30 | 1.81 | 0.00 | Pre-1940 channel |
| S1 | 0.1 | 1.3 | 3.0 | 4.8 | 5.8 | 3.0 | 3.03 | 1.74 | 0.00 | Modern channel |
| S2 | 0.1 | 1.0 | 2.1 | 3.3 | 4.0 | 2.1 | 2.13 | 1.17 | 0.01 | Modern channel |
| S3 | 0.0 | 0.9 | 2.1 | 3.4 | 4.3 | 2.1 | 2.13 | 1.28 | 0.03 | Modern channel |
| S4 | 0.1 | 0.9 | 2.2 | 3.4 | 4.2 | 2.2 | 2.16 | 1.25 | −0.03 | Modern channel |
| S5 | −0.5 | 0.4 | 1.7 | 3.0 | 3.8 | 1.7 | 1.70 | 1.30 | −0.01 | Modern channel |
| S6 | 0.3 | 1.1 | 2.3 | 3.6 | 4.4 | 2.3 | 2.33 | 1.25 | 0.03 | Modern channel |
| S7 | 0.1 | 0.9 | 2.0 | 3.2 | 4.0 | 2.0 | 2.03 | 1.17 | 0.03 | Modern channel |
| S8 | −1.1 | −0.4 | 1.0 | 2.3 | 3.2 | 1.0 | 0.97 | 1.33 | −0.01 | Modern channel |
| S9 | −3.7 | −2.2 | 0.0 | 2.3 | 3.5 | 0.0 | 0.03 | 2.22 | 0.00 | Modern channel |
| S10 | −4.0 | −2.6 | −0.7 | 1.2 | 2.3 | −0.7 | −0.70 | 1.90 | −0.02 | Modern channel |
| S11 | −1.5 | −0.5 | 1.2 | 3.0 | 3.9 | 1.2 | 1.23 | 1.70 | 0.01 | Modern channel |
| S12 | −3.0 | −2.0 | −0.3 | 1.4 | 2.4 | −0.3 | −0.30 | 1.75 | 0.00 | Modern channel |
| S13 | −1.2 | 0.3 | 1.0 | 2.4 | 3.2 | 1.0 | 1.23 | 1.35 | 0.17 | Modern channel |
| S14 | −1.9 | −0.7 | 1.2 | 3.1 | 4.0 | 1.2 | 1.20 | 1.84 | −0.03 | Modern channel |
| S15 | −0.8 | 0.2 | 1.7 | 3.3 | 4.2 | 1.7 | 1.73 | 1.54 | 0.02 | Modern channel |
| S16 | −0.7 | 0.3 | 1.8 | 3.2 | 4.1 | 1.8 | 1.76 | 1.46 | −0.04 | Modern channel |
| S17 | −2.6 | −0.9 | 1.9 | 4.7 | 6.3 | 1.9 | 1.90 | 2.75 | −0.01 | Modern channel |
| S18 | −5.3 | −4.1 | −1.8 | 0.6 | 2.0 | −1.8 | −1.77 | 2.29 | 0.03 | Modern channel |
| S19 | −4.0 | −2.4 | −0.1 | 2.4 | 3.6 | −0.1 | −0.03 | 2.35 | −0.01 | Modern channel |
| S20 | −3.1 | −2.2 | 0.2 | 2.3 | 3.4 | 0.2 | 0.10 | 2.11 | −0.04 | Modern channel |
| S21 | −2.8 | −1.4 | 0.3 | 2.2 | 3.2 | 0.3 | 0.37 | 1.81 | 0.01 | Modern channel |

**Explanation:** "Pre-1935 channel" is older than 1935, and probably formed in 1913. "Pre-1940 channel" existed in 1935 imagery, but was abandoned before 1940 imagery. See text for discussion.

### 4.2. Chronology of Channel Cut-Offs

This study identified three oxbows using historical aerial imagery. Two of the oxbows pre-date the oldest available imagery in 1935. It cannot be certain exactly when either of these oxbows formed. The two most likely candidates for channel cut-offs were the historical floods of 16 March 1913 or 16 January 1930. Of these two, the historical flood of 1913 has been described as a channel-forming event because it was a 500-year flood which devastated wide portions of 12 states throughout the mid-continental region of the United States. The 1913 flood destroyed dams, bridges, and property; killed hundreds of people; and cut off and isolated towns sheltering flood survivors for weeks. Deposits of flood debris from the 1913 flood include trace element geochemical markers derived from industrial chemicals released from ruined factories [36], and flood deposits containing boards, railroad ties, bricks, and other large anthropogenic materials [16]. In this study, the possible 1913 flood deposits found in these two abandoned channels include wood and shell fragments with anomalously old $^{14}C$ ages, which we interpret to represent reworked materials eroded from deposits upstream.

The third oxbow can be more reliably established because it was part of the active channel on 1935 imagery but became an abandoned channel prior to the collection of the 23 May 1940 imagery. The most likely flood of record causing such major channel reorganization occurred on 5 March 1940. The deposits in this abandoned channel include wood debris with a $^{14}C$ calibrated age of 1922, indicating that there was an approximately 18-year response time between the death of the source tree, and deposition of the large wood debris at the base of the abandoned channel succession at this site.

### 4.3. Formation of Fluvial Pavements

This study has found significant historical changes in the textures of channel substrates through the history of urbanization of the watershed. This trend can be discerned looking at any textural parameter, but this discussion will focus on the maximum grain-size component, using the 5$^{th}$ percentile of the cumulative frequency plot in phi units, or $\phi_5$ (**Table 5**). The maximum grain-size class significantly impacts the hydraulic and ecological properties of the channel. The channel substrates in the pre-1935 (most likely 1913) abandoned channels have $\phi_5$ values of +0.78$\phi$. The channel substrates in the 1940 abandoned channel have a $\phi_5$ value of −1.15$\phi$. The modern channel substrates have a $\phi_5$ value of −1.69$\phi$. Collectively, this represents a historical trend of channel substrate coarsening from coarse-grained sand, to granules, to granule-pebble size classes.

In addition to quantitative grain size changes, modern channel sediments are more typically negatively skewed (**Table 5**). Qualitatively, modern channel sediments contain more anthropogenic materials, such as gravel-sized pieces of bricks, concrete, and glass bottles [14] [16].

Channel armoring, or the formation of fluvial pavements, is typically considered evidence of channel incision [37]. Fluvial pavements are commonly found in urban rivers [38] [39]. Our studies on another urban river, the Ottawa River in northern Ohio, have suggested an alternative explanation—urbanization of drainage systems is contributing more stormwater run-off to these channels [14]. Urbanization of storm water run-off is due to the construction of streets, parking lots, housing developments, apartment complexes, commercial districts, and light industry; all having connection to storm sewer systems [40]. The effect of urbanized drainage systems is a shortened lag time and increase in maximum discharge following a rainfall event, resulting in an increase in transport conveyance capacity and hence channel degradation [14] [41].

## 4.4. Sediment Budgets

One approach to understanding historical changes in rivers uses sediment budgets [14] [16]. Land clearance for agriculture created soil erosion and significantly increased sediment inputs into any adjacent fluvial system [42]. Because increased sediment loads typically overwhelmed the sediment conveyance capacity of the fluvial system, legacy sediment accumulated in intrabasinal storage. The physical manifestation of this was vertical aggradation of floodplains, infilling of riparian wetlands, trapping of sediment in reservoirs, and accelerated subsidence [14] [16] [43] [44] [45]. In the study area, land clearance for agriculture started in 1880s-1890s, peaked in 1900-1920, and then declined significantly since 1920 (**Figure 2**).

Urbanization also significantly increases sediment inputs into any adjacent fluvial system, in many cases introducing orders of magnitude more sediment than agricultural practices [40] [44] [46]. However, urbanization is a special case for sediment budgets for two reasons. First, the increased sediment inputs from land clearance for housing developments coincided with hydrologic modifications such as construction of impermeable surfaces and routing of runoff through urban storm-drain networks that increased runoff [40] [47] [48], increased peak streamflow discharge [49] [50] and caused changes in channel morphology [38] [51]. Thus, increased transport conveyance capacity from urbanized storm water run-off systems may have masked the effects of increased sediment input from land clearance. Second, unlike the continuous effect of soil erosion from agricultural fields, sediment input from land clearance for housing developments is more episodic and short-term, because urbanization becomes completed in a region and the disturbed land is revegetated [14] [16]. Thus, after the initial pulse of sediment from land clearance for housing developments, the long-term effects of urbanization may be an increase in transport conveyance capacity (due to more efficient urban storm water drainage systems), and resulting bank erosion, incision, and reworking of sediment held in intrabasinal storage [14] [16].

In summary, many drainage basins in eastern North America show two historical trends: 1) increased sediment inputs due to land clearance for agriculture, overwhelming transport conveyance capacity and resulting in increased intrabasinal storage; followed by 2) reductions in sediment intrabasinal storage due to some combination of more efficient urban storm water run-off systems, abandonment and revegetation of farm fields, improved soil conservation practices, and/or revegetation of disturbed urban areas as a historical wave of suburban housing development reaches completion. During the latter phase, increased transport capacity results in channel incision, terrace formation, and channel bed armoring, bank erosion, and remobilization of legacy sediments that accumulated in intrabasinal storage [14] [16].

This study observed an earlier (pre-1940) phase of cut-offs, channel abandonment, and infill of abandoned channels, followed by a later (post-1940) phase of increased channel sinuosity, channel bed armoring, and bank erosion. These historical changes in Swan Creek correspond to a transition of the drainage basin from: 1) a fluvial system dominated by high sediment inputs due to soil erosion from agricultural land clearance, overwhelmed transport conveyance capacity, and increasing sediment intrabasinal storage (manifest as vertically aggrading floodplains and infilled riparian wetlands); to 2) a fluvial system dominated by increased urban storm water drainage, increased transport conveyance capacity, and decreased sediment intrabasinal storage (manifest as anthropogenic terrace formation, channel degradation, increased lateral channel migration, bank erosion and slumping). High sediment loads and channel bank instability will continue until such time as the fluvial system has removed legacy sediment that accumulated in intrabasinal storage [14] [16].

## 5. Summary and Conclusions

This study used historical aerial imagery and maps to evaluate changes in an urbanized fluvial system in northwestern Ohio (USA). Three abandoned channel complexes were identified on imagery and then in the field. Two abandoned channels pre-date the oldest (1935) imagery but most likely formed as a result of the channel forming discharge of the historical 1913 flood, a 500-year hydrologic event. These 1913 cut-offs contain wood and shell materials with very old $^{14}C$ ages, which is explained as reworked materials eroded from the upstream reaches in this major flood event. The third abandoned channel appears between 1935 and 1940 imagery, and most likely resulted from the historical 1940 flood of record. This abandoned channel contains wood with $^{14}C$ age of 1922, implying the age of the deposit lags the age of the wood by 18 years, and explained as the response time for the wood to move from its site of origin to the site of final deposition.

Sediment cores and trenches facilitated facies analysis of the deposits. In the abandoned channels, channel-fill sands and gravels overlie a basal scour, and represent the bedload that traveled through active channel cross-sections prior to channel abandonment. After channel cut-off occurred, the abandoned channels were infilled by a succession of oxbow lake, riparian wetland, and overbank deposits. Grain size analyses indicate a historical trend of coarsening of the channel substrate over time, from sand-rich to gravel-rich. This is interpreted as evidence of channel armoring, fluvial pavements, and incision. The historical imagery also shows an increase in channel sinuosity over time.

The data are interpreted to show this fluvial system transitioned from an initial natural state (not observed in the data), to an aggradational system pre-1940 due to high amounts of sediment input from land clearance and soil erosion from agricultural fields. During this interval, the channel substrate was sand bed, channel cut-offs and abandonment occurred, there was vertical floodplain aggradation, infilling of abandoned channels, and infilling of riparian wetlands. The fluvial system became degradational post-1940, due to increased storm water discharge from urbanized portions of the drainage basin. During this interval, the channel substrate became gravel, the channel incised, the earlier floodplain became an anthropogenic terrace, bank erosion and slumping increased, and increased lateral channel migration resulted in increased sinuosity. This current trend is projected to continue until the fluvial system re-equilibrates channel morphology with imposed sediment load, by removing all or most of the legacy sediment accumulated in intrabasinal storage.

## Acknowledgements

We wish to thank numerous colleagues for their support in this study. We thank our colleagues in the Department of Geology at Bowling Green State University, especially Jeff Snyder, Sheila Roberts, and Enrique Gomezdelcampo for technical advice. Todd Crail at the University of Toledo identified freshwater bivalves collected in this study. Mark Potucek, Heather Kish, and the vibracoring crew assisted with field work and Nathan Grove with computer support. This study received funding from Bowling Green State University and the BGSU Department of Geology. This paper benefitted from advice from anonymous reviewers.

## Conflicts of Interest

The authors declare no conflicts of interest regarding the publication of this paper.

## References

[1] Hooke, J.M. (1995) River Channel Adjustment to Meander Cutoffs on the River Bollin and River Dane, Northwest England. *Geomorphology*, **14**, 235-253. https://doi.org/10.1016/0169-555X(95)00110-Q

[2] Dieras, P.L., Constantine, J.A., Hales, T.C., Piégay, H. and Riquier, J. (2013) The Role of Oxbow Lakes in the Off-Channel Storage of Bed Material along the Ain River, France. *Geomorphology*, **188**, 110-119. https://doi.org/10.1016/j.geomorph.2012.12.024

[3] Wren, D.G., Davidson, G.R., Walker, W.G. and Galicki, S.J. (2008) The Evolution of an Oxbow Lake in the Mississippi Alluvial Floodplain. *Journal of Soil and Water Conservation*, **63**, 129-135. https://doi.org/10.2489/jswc.63.3.129

[4] Citterio, A. and Piégay, H. (2008) Overbank Sedimentation Rates in Former Channel Lakes: Characterization and Control Factors. *Sedimentology*, **56**, 461-482. https://doi.org/10.1111/j.1365-3091.2008.00979.x

[5] Minderhoud, P.S.J., Cohen, K.M., Toonen, W.H.J., Erkens, G. and Hoek, W.Z. (2016) Improving Age-Depth Models of Fluvio-Lacustrine Deposits Using Sedimentary Proxies for Accumulation Rates. *Quaternary Geochronology*, **33**, 35-45. https://doi.org/10.1016/j.quageo.2016.01.001

[6] Allen, J.R.L. (1965) A Review of the Origin and Characteristics of Recent Alluvial Sediments. *Sedimentology*, **5**, 89-191. https://doi.org/10.1111/j.1365-3091.1965.tb01561.x

[7] Kraus, M.J. and Davies-Vollum, S. (2004) Mudrock-Dominated Fills Formed in Avulsion Splay Channels: Examples from the Willwood Formation, Wyoming. *Sedimentology*, **51**, 1127-1144. https://doi.org/10.1111/j.1365-3091.2004.00664.x

[8] Schumm, S.A. (1977) Patterns of Alluvial Rivers. *Annual Review of Earth and Planetary Sciences*, **13**, 5-27. https://doi.org/10.1146/annurev.ea.13.050185.000253

[9] Erskine, W., McFadden, C. and Bishop, P. (1992) Alluvial Cutoffs as Indicators of Former Channel Conditions. *Earth Processes and Landforms*, **17**, 23-37. https://doi.org/10.1002/esp.3290170103

[10] Mansuy, L., Bourezgui, Y., Garnier-Zarli, E., Jarde, E. and Reveille, V. (2001) Characterization of Humic Substances in Highly Polluted River Sediments by Pyrolysis Methylation-Gas Chromatography-Mass Spectrometry. *Organic Geochemistry*, **32**, 223-231. https://doi.org/10.1016/S0146-6380(00)00169-8

[11] Piégay, H., Bornette, G. and Grante, P. (2002) Assessment of Silting-Up Dynamics of Eleven Cut-Off Channel Plugs on a Free-Meandering River (Ain River, France). In: Allison, R.J., Ed., *Applied Geomorphology*: *Theory and Practice*, John Wiley & Sons, Hoboken, 227-247.

[12] Davidson, G.R., Carnley, M., Lange, T., Galicki, S.J. and Douglas, A. (2004) Changes in Sediment Accumulation Rate in an Oxbow Lake Following Late 19th Century Clearing of Land for Agricultural Use: A $^{210}$Pb, $^{137}$Cs, and $^{14}$C Study in Mississippi, USA. *Radiocarbon*, **46**, 755-764. https://doi.org/10.1017/S0033822200035797

[13] Murphy, R.P., Gomezdelcampo, E. and Evans, J.E. (2007) Using Pre-Existing Channel Substrate to Determine the Effectiveness of Best Management Practices, Sandusky River, Ohio. *Journal of Great Lakes Research*, **33**, 167-181. https://doi.org/10.3394/0380-1330(2007)33[167:UPCSTD]2.0.CO;2

[14] Evans, J.E., Harris, N. and Webb, L.D. (2013) The Shortcomings of "Passive" Urban River Restoration after Low-Head Dam Removal, Ottawa River (Northwestern Ohio, USA): What The Sedimentary Record Can Teach Us. In: DeGraff, J.V. and Evans, J.E., Eds., *The Challenges of Dam Removal and River Restoration*, Vol. 21, Geological Society of America, Boulder, 161-182. https://doi.org/10.1130/2013.4121(13)

[15] Klotz, J.A. and Forsyth, J.L. (1993) Late Glacial Origin of the Maumee Valley Terraces, Northwestern, Ohio. *Ohio Journal of Science*, **93**, 126-133.

[16] Webb-Sullivan, L.D. and Evans, J.E. (2014) Sediment Budget Approach to Understanding Historical Stages of the Ottawa River in the Context of Land-Use Change, Northwestern Ohio and Southeastern Michigan, USA. *Anthropocene*, **7**, 42-56. https://doi.org/10.1016/j.ancene.2015.03.005

[17] Toledo Blade (1961, April 5) City to Acquire Land for Park on Swan Creek.

[18] Howe, H. (1907) Historical Collections of Ohio. The State of Ohio, Cincinnati.

[19] Fisher T.G., Anderson, B. and Stierman, J. (2015) Evidence and Sequence of Ance-

stral Lake Erie Lake-Levels, Northwest Ohio. *Ohio Journal of Science*, **115**, 62-78. https://doi.org/10.18061/ojs.v115i2.4614

[20] USDA (United States Department of Agriculture) (2016) Web Soil Survey Maps. United States Department of Agriculture, Natural Resources Conservation Service, Washington, D.C. https://websoilsurvey.sc.egov.usda.gov

[21] Wilhelm, P.W. (1984) Draining the Black Swamp: Henry and Wood Counties, Ohio, 1870-1920. *Northwest Ohio Quarterly*, **56**, 79-95.

[22] Wikipedia (2016) The Great Black Swamp. https://en.wikipedia.org/wiki/Great_Black_Swamp

[23] Brewer, L.G. and Vankat, J.L. (2004) Description of Vegetation of the Oak Openings of Northwestern Ohio at the Time of Euro-American Settlement. *The Ohio Journal of Science*, **104**, 76-85.

[24] Hicks J.L. (2017) Oxbow Lakes as Geological Archives of Historical Changes in Channel Substrate; Swan Creek Metropark, Toledo, Ohio. M.S. Thesis, Bowling Green State University, Bowling Green, 167 p. https://doi.org/10.1130/abs/2017NE-290759

[25] Goddard, E.N., Trask, P.D., Deford, R.K., Rove, O.N., Singewald, J.T. and Overbeck, R.M. (1948) Rock-Color Chart. Geological Society of America, Boulder.

[26] Folk, R.L. (1974) Petrology of Sedimentary Rocks. Hernphill Publishing Co., Austin, 194 p.

[27] Faure, G. and Mensing, T.M. (2005) Isotope Principle and Applications, 3rd Edition. John Wiley & Sons, Hoboken, 614 p.

[28] Stuiver, M. and Reimer, P.J. (1993) Extended $^{14}C$ Data Base and Revised CALIB 3.0 $^{14}C$ Age Calibration Program. *Radiocarbon*, **35**, 215-230. https://doi.org/10.1017/S0033822200013904

[29] Reimer, P., Bard, E., Bayliss, A., Beck, J., Blackwell, P., Ramsey, C., et al. (2013). IntCal13 and Marine13 Radiocarbon Age Calibration Curves 0 - 50,000 Years cal BP. *Radiocarbon*, **55**, 1869-1887. https://doi.org/10.2458/azu_js_rc.55.16947

[30] Esri (2017) ArcGIS Slope Spatial Analyst. http://desktop.arcgis.com/en/arcmap/10.3/tools/spatial-analyst-toolbox/slope.htm

[31] Hughes, M.L., McDowell, P.F. and Marcus, A.W. (2006) Accuracy Assessment of Georectified Aerial Photographs: Implications for Measuring Lateral Channel Movement in a GIS. *Geomorphology*, **74**, 1-16. https://doi.org/10.1016/j.geomorph.2005.07.001

[32] Esri (2016) ArcGIS Data Classification Methods. http://pro.arcgis.com/en/proapp/help/mapping/symbols-and-styles/data-classification-methods.htm

[33] McCabe, P.J. (1984) Depositional Environments of Coal and Coal-Bearing Strata. In: Rahrnani, R.A. and Flores, R.M., Eds, *Sedimentology of Coal and Coal-Bearing Sequences*, Special Publication No. 7, International Association of Sedimentologists, Oxford, 13-42.

[34] Walker, R. G. and Cant, D.J. (1984) Sandy Fluvial Systems In: Walker, R.G., Ed., *Facies Models,* 2nd Edition, Geoscience Canada Reprint Series 1, Geological Association of Canada, Newfoundland, 71-89.

[35] Toonen, W.H.J., Kleinhans, M.G. and Cohen, K.M. (2012) Sedimentary Architecture of Abandoned Channel Fills. *Earth Surface Processes and Landforms*, **37**, 459-472. https://doi.org/10.1002/esp.3189

[36] Peck, J.A., Mullen, A., Moore, A. and Rumschlag, J.H. (2007) The Legacy Sediment

Record within the Munroe Falls Dam Pool, Cuyahoga River, Summit County, Ohio. *Journal of Great Lakes Research*, **33**, 127-141.
https://doi.org/10.3394/0380-1330(2007)33[127:TLSRWT]2.0.CO;2

[37] Julien, P.Y. and Anthony D.J. (2002) Bed Load Motion and Grain Sorting in a Meandering Stream. *Journal of Hydraulic Research*, **40**, 125-133.
https://doi.org/10.1080/00221680209499855

[38] Pizzuto, J.E., Hession, W.C. and McBride, M. (2000) Comparing Gravel-Bedded Rivers in Paired Urban and Rural Catchments of Southeastern Pennsylvania. *Geology*, **28**, 79-82.
https://doi.org/10.1130/0091-7613(2000)028%3C0079:CGRIPU%3E2.0.CO;2

[39] Poleto, C. and Merten, G.H. (2007) Urban Watershed Studies in Southern Brazil. *Journal of Urban and Environmental Engineering*, **1**, 70-78.

[40] Wolman, M.G. and Schick, A.P. (1967) Effects of Construction on Fluvial Sediment, Urban and Suburban Areas of Maryland. *Water Resources Research*, **3**, 451-464.
https://doi.org/10.1029/WR003i002p00451

[41] Harris, N. and Evans, J.E. (2014) Channel Evolution of Sandy Reservoir Sediments Following Low-Head Dam Removal, Ottawa River, Northwestern Ohio, USA *Open Journal of Modern Hydrology*, **4**, 44-56.
https://doi.org/10.4236/ojmh.2014.42004

[42] Jacobson, R.B. and Coleman, D.J. (1986) Stratigraphy and Recent Evolution of Maryland Piedmont Flood Plains. *American Journal of Science*, **286**, 617-637.
https://doi.org/10.2475/ajs.286.8.617

[43] Walter, R.C. and Merritts, D.J. (2008) Natural Streams and the Legacy of Water-Powered Mills. *Science*, **319**, 299-304. https://doi.org/10.1126/science.1151716

[44] Allmendinger, N.E., Pizzuto, J.E., Moglen, G.E. and Lewicki M. (2007) A Sediment Budget for an Urbanizing Watershed, 1951-1996, Montgomery County, Maryland, USA. *Journal of the American Water Resources Association,* **43**, 1483-1498.
https://doi.org/10.1111/j.1752-1688.2007.00122.x

[45] Kroes, D.E. and Hupp, C. (2010) The Effect of Channelization on Floodplain Sediment Deposition and Subsidence along the Pocomoke River, Maryland. *Journal of the American Water Resources Association*, **46**, 686-699.
https://doi.org/10.1111/j.1752-1688.2010.00440.x

[46] Gellis, A.C., Webb, R.M.T., Wolfe, W.J. and McIntyre, S.C.I (1996) Land Use, Upland Erosion, and Reservoir Sedimentation, Lago Loiza, Puerto Rico. *Geological Society of America*, *Abstracts with Programs*, **28**, Article No. 79.

[47] Carter, R.W. (1961) Magnitude and Frequency of Floods in Suburban Areas. Professional Paper 424-B, U.S. Geological Survey, Reston, 9-11

[48] Booth, D.B. and Jackson, C.R. (1997) Urbanization of Aquatic Systems: Degradation Thresholds, Stormwater Detention, and the Limits of Mitigation. *Journal of the American Water Resources Association*, **33**, 1077-1090.
https://doi.org/10.1111/j.1752-1688.1997.tb04126.x

[49] Beighley, E. and Moglen, G.E. (2003) Adjusting Peak Discharges from an Urbanizing Watershed to Reflect a Stationary Land Use Signal. *Water Resources Research*, **39**, Article No. 1093. https://doi.org/10.1029/2002WR001846

[50] Meierdiercks, K.L., Smith, J.A., Baeck, M.L. and Miller, A.J. (2010) Heterogeneity of Hydrologic Response in an Urban Watershed. *Journal of the American Water Resources Association*, **46**, 1221-1237.
https://doi.org/10.1111/j.1752-1688.2010.00487.x

[51] Segura, C. and Booth, D. (2010) Effects of Geomorphic Setting and Urbanization on Wood, Pools, Sediment Storage, and Bank Erosion in Puget Sound Streams. *Journal of the American Water Resources Association*, **46**, 972-986. https://doi.org/10.1111/j.1752-1688.2010.00470.x